High Shear Skim Milk Ultrafiltration Using Rotating Disk Filtration Systems

Lu-Hui Ding, Omar Akoum, Antoine Abraham, and Michel Y. Jaffrin
Technological University of Compiegne, UMR CNRS 6600, 60205 Compiegne, France

The ultrafiltration (UF) of UHT (sterilized at ultrahigh temperature) skim milk with two prototypes rotating disk systems of 15.5 and 26 cm i.d. using the same 50 kDa PES membrane is investigated. The larger stainless steel unit had a maximum rotation speed of 1,500 rpm. The smaller nylon unit had a maximum speed of 3,000 rpm. Disks equipped with radial vanes of various heights were used in the tests. The large module yielded a stabilized permeate flux of 276 L $h^{-1}m^{-2}$ at 45°C and a transmembrane pressure (TMP) of 1,000 kPa when fitted with a 2-mm vanes disk rotating at 1,500 rpm, confirming the reduction of concentration polarization by high shear rate. The mean shear rate on membrane γ_m was shown to be proportional to $(k\omega)^{1.8}$, where ω was the disk angular velocity and k was a coefficient depending upon vanes height. Permeate fluxes observed with the two modules at various speeds and with different disks were well correlated by a single function of mean shear rate, given in $Lh^{-1}m^{-2}$ by $J = 0.301\ \gamma_m^{0.552}$. In concentration tests with a 6-mm vanes disk, the permeate flux remained constant until a volume reduction ratio (VRR) of 3, then decayed to a theoretical VRR maximum of 9.2 at zero flux. It can thus be concluded that rotating disk filtration devices are very efficient in UF as high shear reduces concentration polarization. The specific power consumed per m^3 of permeate was found to be less for the smooth disk than for a disk with vanes.

Introduction

The dairy industry makes extensive use of ultrafiltration (UF) for concentrating total milk proteins in cheese production or for protein concentration standardization (Maubois et al., 1971; Ernstrom et al., 1980; Grandison et al., 2000). Recently, UF has been proposed to separate α-lactalbumine from β-lactoglobulin (Lucas et al., 1998). However, protein transmission was hindered by membrane fouling due to micelle casein layer deposited on the membrane. Thus, it seems legitimate to evaluate the suitability of dynamic or shear-enhanced filtration to these applications.

In three recent articles, Al-Akoum et al. (2002a,b, 2003) have investigated the performance of a Vsep shear-enhanced dynamic filtration device for concentrating proteins in UHT milk (sterilized at ultra high temperature) by UF and separating casein micelles from whey proteins by microfiltration (MF) and UF. When using a 0.1 μm membrane, the permeate flux reached a plateau of 95 L $h^{-1}m^{-2}$ at a mean transmembrane pressure (TMP) of 100 kPa at initial concentration, a temperature of 45°C and maximum frequency, higher than those reported in the literature using tubular ceramic membranes of same pore size (Gésan-Guiziou et al., 2002). In UF with a 50 kDa membrane, the permeate flux reached 80 L $h^{-1}m^{-2}$ at a TMP of 600 kPa, at maximum frequency. Similarly, when equipped with a 50 kDa membrane, the Vsep was able to reach a volume reduction ratio (VRR) of 8.66 (Al-Akoum et al., 2002a), higher than that reported in conventional cross-flow filtration. The good performance of the Vsep can be attributed to the high shear rate at the membrane induced by the rapid oscillating azimuthal motion of the membrane reaching an amplitude of 30 mm at periphery, at a resonant frequency of 60.75 Hz. With milk, the time maximum shear rate at membrane was calculated to be 10^5 s^{-1} at periphery and 7×10^4 s^{-1} when averaged over the membrane area.

In this article, we investigate the performance in milk ultrafiltration of another dynamic filtration system consisting in

Correspondence concerning this article should be addressed to M. Y. Jaffrin.

a disk rotating at high speed near a circular membrane. Such systems, which are commercially available both as laboratory pilots and industrial units, have been shown to be very efficient, especially in macromolecule recovery from cell suspensions (Lee et al., 1995; Frenander and Jönsson, 1996; Pessoa and Vitolo, 1998; Harscoat et al., 1999). A survey of commercial rotating disk systems has been made by Bouzerar et al. (2000). On using several small pilots with disks equipped with vanes designed and built in our laboratory (Bouzerar et al., 2000; Brou et al., 2002), we have shown that the presence of vanes greatly increased the performance both in terms of permeate flux and of the energy consumed by the disk per m^3 of permeate. However, most applications of these rotating disk systems were in the field of microfiltration, because of highly reduced cake formation in these devices. One of the few UF applications reported was that of Dal-Cin et al. (1998) who used a Spintek system with a 500 cm^2 (28 cm dia.) membrane mounted on the rotating disk for UF of oil-water microemulsions. However, since the permeate pressure increased with rotation speed due to centrifugal forces, reducing the effective mean transmembrane pressure (TMP), the permeate flux reached a peak at 1,000 rpm, and the full potential of the system could not be exploited.

Our system, which features a fixed membrane, does not suffer from this limitation. In addition we built a stainless steel module capable of reaching pressure of more than 1,500 kPa, in order to reach the pressure-independent plateau for the flux which occurred at high TMP since concentration polarization was reduced by the high shear.

Materials and Methods

Rotating disk systems

These systems were designed in our laboratory. The smaller modules, described by Bouzerar et al. (2000), consisted in a cylindrical housing of an inner radius $R = 0.0775$ m. The unit used in this study was machined from stainless steel and featured an aluminum disk of radius $R_d = 0.0725$ m rotating at adjustable speed up to 3,000 rpm around a horizontal shaft (Figure 1). A 190 cm^2 polyethersulfone (PES) 50 kDa fixed membrane, supported by a 0.3 mm thick polypropylene grid, was mounted on the flat front end of the housing, while the milk was fed through the back plate on the other side of the disk. It is then centrifuged by the disk to the rim and over the membrane side and recirculates between the membrane and disk, before being evacuated through the hollow shaft. The gap (e) between the membrane and the disk was 15 mm. Permeate was collected from a tap located at the top of the front plate. The permeate flow rate was measured by collecting the permeate in a beaker continuously weighted on an electronic scale (Sartorius, Germany) connected to a microcomputer calculating the derivative of the collected volume with respect to time and providing a value of flux every 10 s if needed. The peripheral pressure was measured at the top of the cylindrical housing by a Validyne DP15 pressure transducer. The test fluid was fed from a 10 L-thermostated reservoir by a volumetric membrane pump at a flow rate of 60 L h^{-1} in all filtration tests in order to be in excess of the highest permeate flow rate encountered. Circuit internal volume was 1 L.

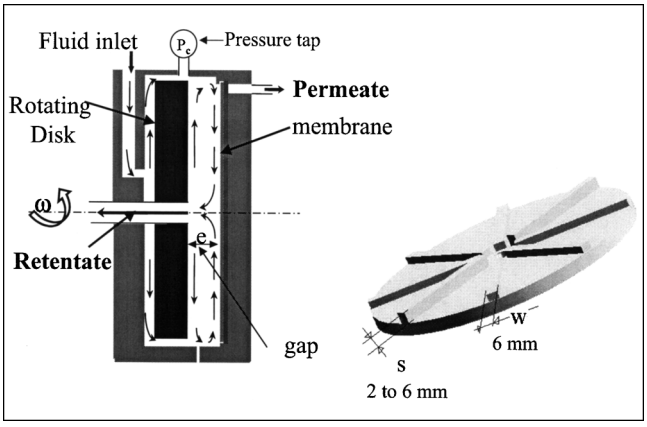

Figure 1. Rotating filtration module.

A larger module (Bouzerar et al., 2001) was built in stainless steel with a 26 cm i.d. housing receiving a 460 cm^2 annular membrane ($R_1 = 0.047$ m, $R_2 = 0.13$ m) of the same material (PES 50 kDa) as in the smaller module. The gap between membrane and disk was 10 mm. Due to technical constraints, only inlet and outlet fluid pressure were measured in this unit. From a comparison made with the small module, it was determined that TMP was equal to inlet pressure. The maximum rotation speed was 1,500 rpm and the inlet flow was 180 L h^{-1}. The tank volume was equal to 15 L and the circuit volume to 3 L.

Several types of disks were used in these units. Initial disks (denoted as smooth) were flat on both sides. Subsequent disks were equipped with eight radial vanes of various heights (s), 2 mm for the large module and 2, 4, and 6 mm for the small one.

Main features of the flow field

The flow field between the membrane and a rotating flat disk has been described previously by Bouzerar et al. (2000). Since the axial gap between the membrane and the disk was relatively large (at least 5 mm), the flow was of a boundary layer type and turbulent except at low speeds and in the central part. It is known (Schlichting, 1968) that the inviscid core between the boundary layers rotates at the angular velocity $k\omega$, lower than the disk angular velocity ω. Thus, the pressure distribution with radius r in the inviscid core is given by Bernoulli's equation

$$p = (1/2)\rho k^2\omega^2 r^2 + p_0 \tag{1a}$$

where p_0, the pressure at the center is also equal to the pressure when the disk is at rest and ρ denotes fluid density. Equation 1a permits us to determine by regression the velocity coefficient k from peripheral pressure measurements taken on the housing rim at various angular velocities. Since the permeate is collected at atmospheric pressure, the TMP in the small module is obtained by integration of Eq. 1a over the membrane as

$$p_{tm} = p_c - (1/4)\rho k^2\omega^2 R_2^2 \tag{1b}$$

Table 1. Internal Dimensions of the Two Modules

Module	R (m)	R_1 (m)	R_2 (m)	R_d (m)
Small	0.0775	—	0.0775	0.0725
Large	0.131	0.047	0.130	0.120

where p_c is the peripheral pressure at $r = R$.

The shear rate on the stationary membrane has been calculated by Bouzerar et al. (2000) in the turbulent regime to be

$$\gamma_{wt} = 0.0296\ \nu^{-0.8}(k\omega)^{1.8} r^{1.6} \qquad (2a)$$

The mean shear rate over the membrane is calculated by integrating Eq. 2a over the membrane up to the disk radius R_d for both units to be given by

$$\gamma_m = 0.0164\ \nu^{-0.8}(k\omega)^{1.8}\left(R_d^{3.6} - R_1^{3.6}\right)/\left(R_d^2 - R_1^2\right) \quad (2b)$$

where the dimensions of R_d and R_1 are given in Table 1 for both modules.

Although Eqs. 2a and 2b have been derived for a flat disk, we will attempt to use them with disks equipped with vanes, but taking the value of k corresponding to these disks.

Test fluid

Since it was readily available, the test fluid was commercial UHT (sterilized at ultra high temperature) skim milk (Printiligne, Patûrages de France). This milk had been sterilized at 140°C for 3 s and had the following characteristics: casein: 25.6 g L^{-1}, whey proteins: 6.4 g L^{-1}, lactose: 46 g L^{-1} and calcium: 1.2 g L^{-1}. According to Miralles et al. (2000), the protein composition of UHT milk is similar to that of pasteurized milk, with a whey protein ratio to total protein of 18–20%, except that whey proteins may be partially denatured, to the rate of 20% for α-lactalbumin and 65% for β-lactoglobulin. The milk temperature was monitored in the tank by a Digitron platinum resistance thermometer (SIFAM Ltd., Torquay, Devon, U.K.). Tests were carried out at initial concentration (VRR = 1) and at VRR = 1.8 and a temperature of 45°C which are standard operating conditions for this process in industry.

The milk pH was measured by a pH-meter Mettler Toledo MP 125 (Switzerland). The average initial pH in the tests was 6.4 and never dropped by more than 0.3, indicating the absence of bacterial development. The milk viscosity μ was measured by a Rheostress Rheometer (Haake, Karlsuche, Germany) thermostated at 45°C with coaxial cylinders at 5,000 s^{-1}, which was the highest shear rate possible. We found that $\mu = 0.98 \times 10^{-3}$ Pa s for VRR = 1, $\rho = 1{,}016$ kg m^{-3} and $\mu = 1.41 \times 10^{-3}$ Pa s for VRR = 1.8, $\rho = 1{,}035$ kg m^{-3}. The permeate was checked for casein micelles using a HACH turbidimeter to ± 1 NTU (Nephelometric Turbidity Unit).

Cleaning procedure

Before and after each test, the circuit was first rinsed with demineralized water, then washed with 5 L of Ultrasil P3-25F solution (0.5% in demineralized water) at 50°C for 15 min and rinsed again with 5 L of demineralized water. A new membrane was used in each test.

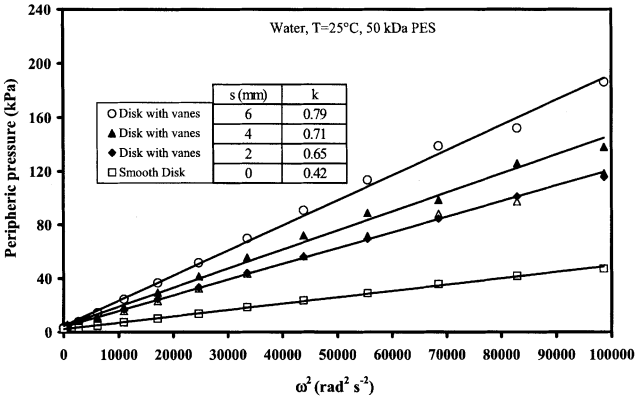

Figure 2. Determination of velocity coefficients of various disks from peripheral pressure measurements as a function of square of angular velocity.

Results

Determination of velocity coefficients

The peripheral pressure of the small module was measured at various rotation speeds from 0 to 3,000 rpm in order to determine velocity coefficients k for various disks from Eq. 1a. It can be seen from Figure 2 that Eq. 1a is well verified and that k is given by the square root of the slopes of the linear correlations. The highest velocity coefficient (0.79) was obtained for 6-mm high vanes. As expected, the smooth disk gives the smallest coefficient (0.42). Only the smooth disk and the disk with 6-mm high vanes were used in tests presented here with the small module. The velocity coefficients of disks in the large module could not be measured as it was not equipped with a peripheral pressure tap, so coefficients measured for vanes of the same height in the small module were used instead. To facilitate comparison between tests performed with the two modules their respective mean membrane shear rates calculated from Eq. 2b are plotted as a function of rotation speed in Figure 3. The highest mean shear rate (2.34×10^5 s^{-1}) was obtained with the small module and a 6-mm vanes disk at 2,500 rpm.

Variation of permeate flux with time with the small module

The variation of permeate flux with time using a smooth disk and TMP of 200 and 300 kPa is shown in Figure 4. Each test started with 5 min of filtration at minimal TMP with the retentate valve fully open. The valve was then tightened progressively to reach the desired TMP. These experiments were repeated with a disk equipped with 6-mm vanes at the same TMP and the corresponding data are also shown in Figure 4 for comparison. While there is a 35% increase in stabilized permeate flux at 300 kPa in the presence of vanes, there is hardly any increase at 200 kPa. This indicates that, at 200 kPa, the flux is governed by pressure and not shear depen-

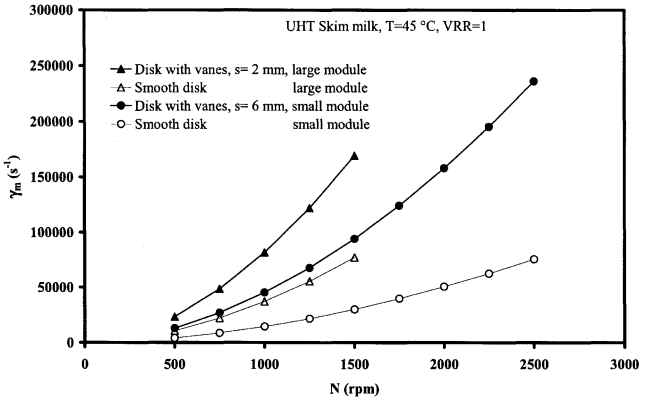

Figure 3. Variation of mean membrane shear rate with rotation speed for the two modules and various disks.

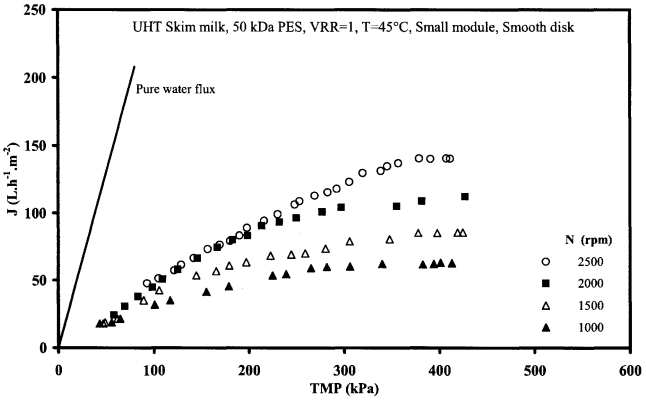

Figure 5. Variation of permeate flux with TMP for a smooth disk at various rotation speeds and VRR = 1 (small module).

From Ding et al. (2002).

dent as in a mass-transfer limited regime. With this disk, the permeate flux decays by 25% from 180 to 130 L h^{-1}m^{-2} at a TMP of 300 kPa in 40 min, but the decay is smaller (18%) at 200 kPa since less proteins are brought to the membrane by the smaller flux.

Variation of permeate flux with TMP at different rotation speeds and VRR = 1

Small Module. Filtration was first carried out at minimal pressure during 30 min to avoid an initial peak for the permeate flux. The TMP was then increased in steps waiting for the flux to stabilize before recording its value. This variation is illustrated in Figure 5 for a smooth disk, together with the pure water flux corresponding to a permeability of 260 L h^{-1}m^{-2} bar^{-1}. The permeate flux reaches a plateau at a TMP of 400 kPa for all speeds above 1,000 rpm and at 300 kPa at 1,000 rpm. This plateau increases from 63 L h^{-1}m^{-2} at 1,000 rpm to 141 L h^{-1}m^{-2} at 2,500 rpm. Permeate turbidity was low at less than 2 NTU, confirming quasi complete retention of casein micelles as expected since the pore diameter was much smaller than the micelle size (20–600 nm).

When the smooth disk is replaced by a disk equipped with 6 mm vanes, the permeate flux shown in Figure 6 remains proportional to TMP and is almost independent of rotation speed up to 450 kPa for speeds equal or higher than 1,500 rpm. The permeate flux reaches a maximum of 213 L h^{-1}m^{-2} at 2,500 rpm and a pressure of 570 kPa.

Large Module. The variation of permeate flux with TMP is shown in Figure 7 for a smooth disk and in Figure 8 for a disk equipped with 2 mm vanes. Since this unit was sturdier than the smaller unit, it could stand higher pressures. At speeds of 1,250 and 1,500 rpm, the maximum flux seems to be reached at higher pressures than with the smaller module at a speed of 2,500 rpm. The maximum flux 276 L h^{-1}m^{-2} was obtained at 1,500 rpm and 1,000 kPa in the large module with 2-mm vanes. This flux is larger than the maximum (213 L h^{-1}m^{-2}) observed at 2,500 rpm in the small module with 6-mm vanes, but at a lower pressure 550 kPa. The corresponding peripheral core fluid velocities $k\omega R_d$ were, respectively, 15.0 and 12.2 m s^{-1} for the small and large modules.

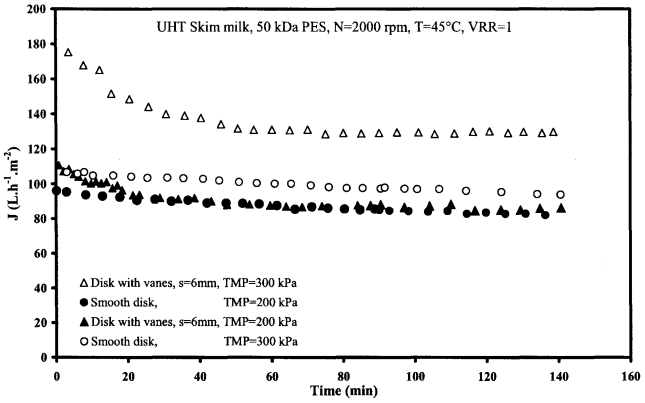

Figure 4. Variation of permeate flux with time at VRR = 1 and a rotation speed of 200 rpm (small module) for two types of disks and TMP of 200 and 300 kPa.

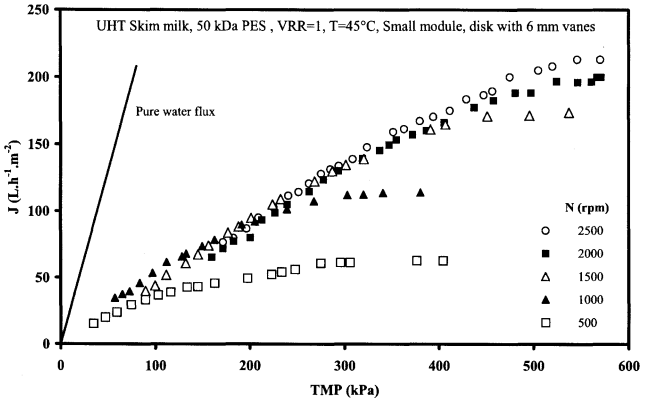

Figure 6. Variation of permeate flux with TMP at various rotation speeds and VRR = 1 (small module) with a disk equipped with 6-mm vanes.

From Ding et al. (2002).

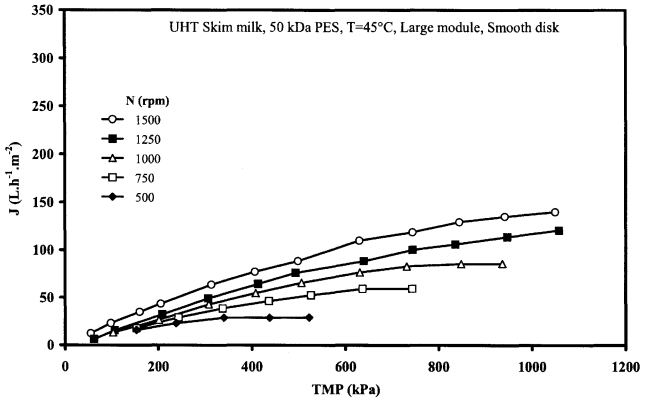

Figure 7. Variation of permeate flux with TMP for a smooth disk at various rotation speeds and VRR = 1 (large module).

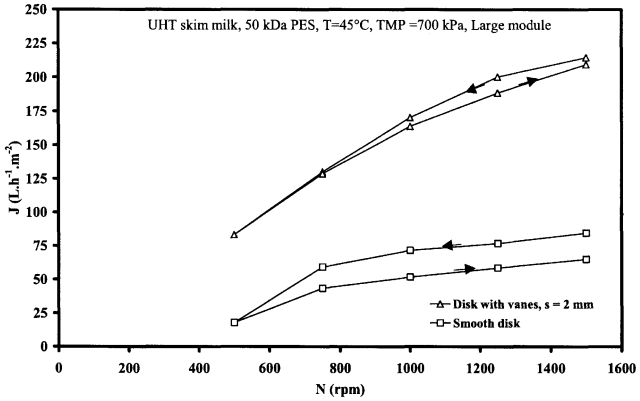

Figure 9. Variation of permeate flux with rotation speed at a TMP of 700 kPa for the large module and two types of disks.

However, it will be seen in the next section that a more meaningful comparison can be made in terms of the membrane mean shear rate.

The advantage of higher TMP is clear in the large module at high shear rates, with a disk equipped with vanes and rotating at high speed. It is clear that concentration polarization is reduced due to very high shear, and the permeate flux reaches its maximum at a higher pressure than in the smooth disk.

The variation of permeate flux, when rotation speed is varied from 1,500 to 500 rpm and raised again to 1,500 rpm over a period of 90 min at a constant TMP of 700 kPa, is plotted in Figure 9 for two types of disks. Each data point corresponds to a stabilized value of the flux. In order to start with stable conditions, filtration was carried out initially for 90 min at 1,500 rpm before reducing the speed. The beneficial effect of vanes on permeate flux is striking. Not only was permeate flux 2.5 times higher with vanes at the initial speed of 1,500 rpm, but the presence of vanes reduced the irreversible fouling in the second part of the test when speed was increased.

Variation of permeate flux with mean membrane shear rate for the two modules and various disks

The maximum permeate fluxes obtained at various rotation speeds from 500 to 2,500 rpm with the two modules with different disks were collected from data of Figures 5 to 8 at VRR = 1 and plotted against the mean membrane shear rate γ_m in Figure 10 with appropriate values of velocity coefficients. It is interesting to observe that permeate fluxes measured in the two modules for disks with and without vanes obey the same correlation in terms of the mean membrane shear rate which is written for VRR = 1 as

$$J = 0.301\ \gamma_m^{0.552} \tag{3}$$

where γ_m is given by Eq. 2b.

We have also included for comparison the corresponding data with the small module obtained at a VRR of 1.8 with 6 mm vanes which vary with almost the same power of the mean

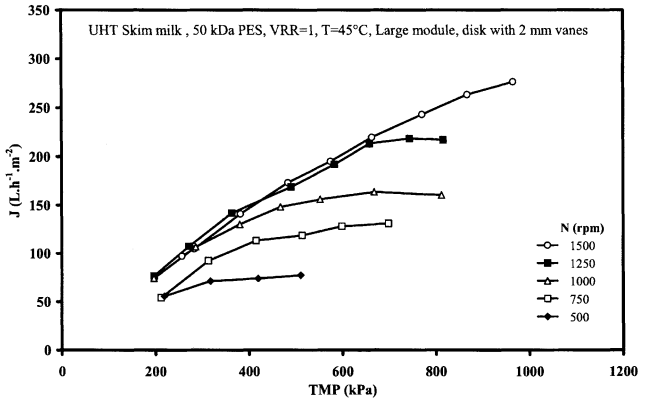

Figure 8. Variation of permeate flux with TMP at various rotation speeds and VRR = 1 (large module) with a disk equipped with 2-mm vanes.

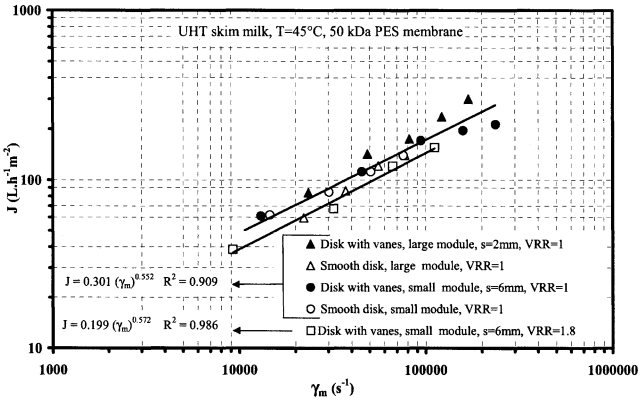

Figure 10. Variation of maximum permeate flux with mean membrane shear rate for the two modules and various types of disks at VRR = 1 and for a 6-mm vanes disk at VRR = 1.8.

membrane shear rate, calculated using viscosity at VRR = 1.8, as

$$J = 0.199\ \gamma_m^{0.572} \tag{4}$$

The numerical coefficient in Eq. 4 is lower than in Eq. 3 as expected, because it depends on diffusivity which is lower at VRR = 1.8.

These results mean that the permeate flux is governed mainly by the mean membrane shear rate and not by details of the internal flow and of the housing or disk geometry. This observation is not in contradiction with the remarks made in the preceding section when the permeate fluxes obtained from the two modules were compared in the light of fluid core velocity. Since the powers of ω and radius are different in Eq. 2b, shear rates may be the same in the two modules when core fluid velocities are different.

Concentration tests

Such tests are normally carried out by recycling the retentate only and not the permeate. However, in order to eliminate the effect of initial fouling noticed in Figure 4, the first 90 min of tests were carried out at initial concentration by recycling the permeate. In addition, during the first 5 min of filtration, the retentate valve was kept open, then it was shut progressively to reach the desired TMP to minimize initial fouling. After 90 min, the permeate recirculation was stopped and the concentration phase was started until the retentate volume became equal to the dead volume in order to reach the maximum value of volume reduction ratio (VRR). The variation of permeate flux with ln(VRR) is displayed in Figure 11 for a smooth disk, TMP of 200 and 300 kPa and a rotation speed of 2,000 rpm. Total duration of the test was 10 h, so each permeate data corresponds to a stabilized value. It is seen that the permeate flux drops slowly below a VRR of 1.3, while, at higher concentrations, it obeys the classical concentration polarization law of the form

$$J = J_0 - K\ \ln\ (\mathrm{VRR}) \tag{5}$$

where J_0 is equal to 98.3 L $h^{-1}m^{-2}$ at 200 kPa and 106.9 L $h^{-1}m^{-2}$ at 300 kPa. Fluxes at VRR $\leq$ 1.3 are lower than these

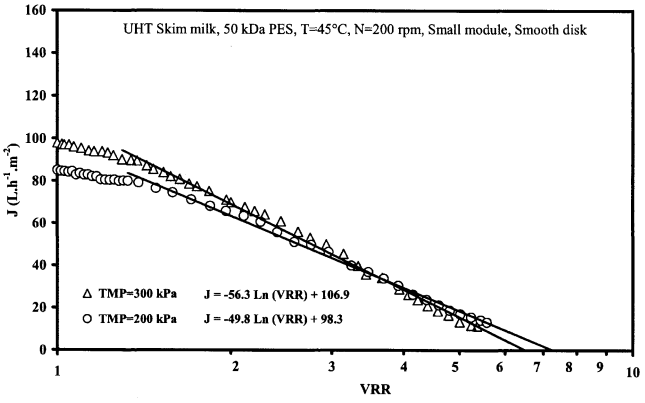

Figure 11. Variation of permeate flux with VRR in semi log coordinates at 2,000 rpm, with a smooth disk and TMP of 200 and 300 kPa (small module).

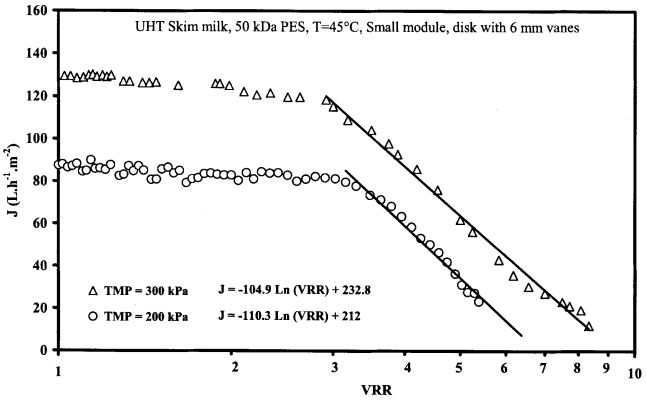

Figure 12. Variation of permeate flux in the VRR in semi-log condensates at 2,000 rpm in the 6-mm vanes at TMP of 200 and 300 kPa (small module).

values since they are not in the mass-transfer limited regime, as it can be inferred from Figure 5. The mass-transfer coefficients K at these two pressures are, respectively, 49.8 and 56.3 L $h^{-1}m^{-2}$. The corresponding maximum VRR obtained by extrapolation to $J = 0$ are 7.2 and 6.7. The variation of permeate flux with concentration was markedly different when a 6-mm vanes disk was fitted in the module (Figure 12). Not only permeate fluxes were higher than with the smooth disk, but they remain practically constant until a VRR of 3, because they correspond to a pressure limited regime, as seen from Figure 6 for VRR = 1. Therefore, Eq. 5 only applies at VRR larger than 3 with mass-transfer coefficients of 110 and 105 L $h^{-1}m^{-2}$ at TMP of 200 and 300 kPa, respectively. The maximum VRR obtained by extrapolation to zero flux were, respectively, 6.8 (200 kPa) and 9.2 (300 kPa). This last figure is much higher than the value of 5.6 observed in cross-flow ultrafiltration with tubular membranes (Bouzaza et al., 1989). With the Vsep system, Al-Akoum et al. (2002a) have observed a theoretical maximum VRR of 8.7 at 400 kPa close to the maximum obtained by the rotating disk with vanes.

The results of a concentration test performed with the large module and a disk equipped with 2-mm vanes at a TMP of 800 kPa are represented in Figure 13. The variation of permeate flux with VRR is similar to that obtained with the small module showing a slow decay with concentration until VRR = 2. The permeate flux during this phase is higher than those of the smaller module even with a 6-mm vanes disk. Above VRR = 2, the permeate flux is mass-transfer limited and decays faster than for the small module. Consequently, the theoretical maximum VRR obtained by extrapolation to zero flux drops to 6.2 vs. 9.2 for the small module with a 6-mm vanes disk. This different behavior may be due to the higher pressure, 800 kPa instead of 300 since mean shear rates are almost the same in both modules in these conditions, as seen from Figure 3.

Energy considerations

Since the energy necessary to drive the disk may be important in industrial sized systems, we have measured the electrical power consumed by our device. However, in order to

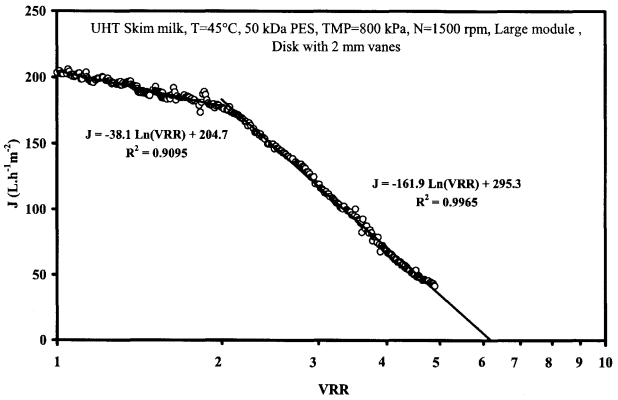

Figure 13. Variation of permeate flux with VRR in semi log coordinates at 1,500 rpm for the large module with a 2-mm vanes disk and TMP of 800 kPa.

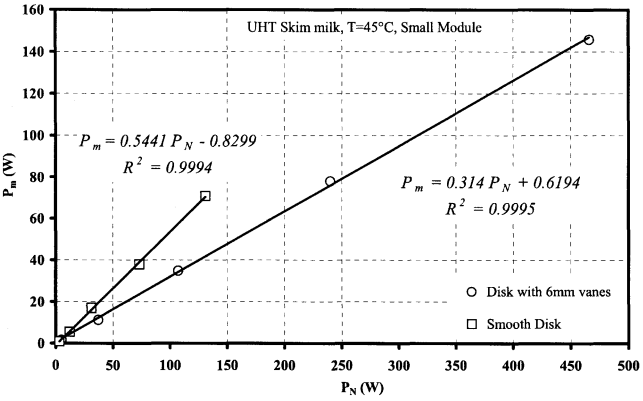

Figure 15. Variation of mechanical power exerted by the disk on the fluid with electrical power consumed.

Slopes of lines correspond to mechanical efficiency of motor-disk system.

eliminate the energy consumed by friction of the rotating shaft, which is disproportionally high in a single membrane device, we have calculated the net power consumed by the disk itself P_N, as described by Brou et al. (2002). To this effect, we have subtracted the power P_{eu} consumed when the module is empty from the power P_e during filtration at the same speed. These net powers are shown in Figure 14 as a function of rotation speed for a smooth disk and a disk with 6-mm vanes together with corresponding values of stabilized fluxes. As expected, the net power increases with the square of rotation speed, faster than the permeate flux. It can be noticed also that the power increase due to the vanes is larger than the corresponding increment in permeate flux.

In order to estimate the mechanical efficiency of our system, we have computed the mechanical power P_m developed by friction forces on the two sides of the disk as

$$P_m = 2\pi \int_0^R (\tau_{dt} + \tau_{db}) r^2 \omega dr \qquad (6)$$

where τ_{db} denotes the shear stress on the smooth back of the disk. The result using Eq. 2a, is

$$P_m = 0.0779\ \rho \nu^{1/5} \omega^{14/5} R_d^{23/5} \left(k^{9/5} + k_0^{9/5}\right) \qquad (7)$$

where k_0 denotes the velocity coefficient for the (flat) back of the disk.

As observed by Brou et al (2002) in the case of MF of yeast suspensions with a similar device, the mechanical power is found in Figure 15 to vary linearly with electrical power supplied to the disk, yielding a mechanical efficiency of 31.4% for a disk equipped with 6 mm vanes and of 54.4% for a smooth disk.

Consequently, the ratio of net power by the maximum permeate flow rate, equal to the electrical energy per m^3 of permeate, which is plotted in Figure 16, is higher for the disk with vanes than for the smooth disk. This situation is opposite to that observed in MF of yeast suspensions (Brou et al., 2002) and of fermentation broths (Brou et al., 2003). The net power consumed by the disk in MF was very close to present

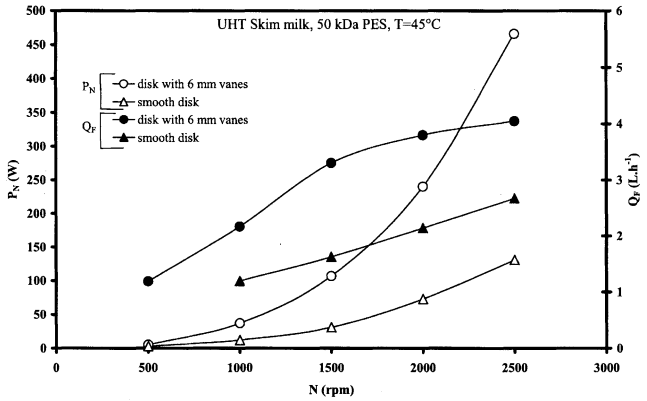

Figure 14. Variation of net power consumed by the disk and permeate flow rate with rotation speed in the small module with a smooth disk and a 6-mm vanes disk.

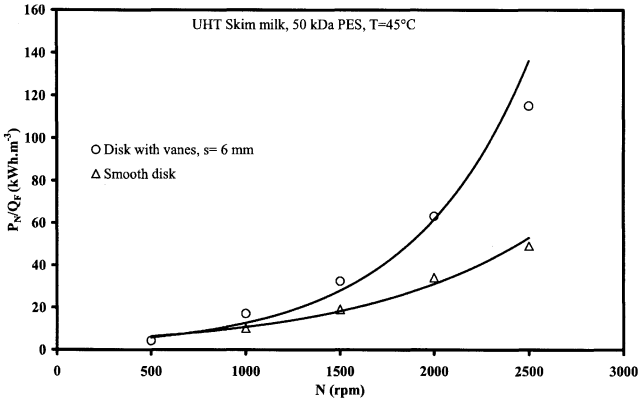

Figure 16. Variations of specific energy consumed by the disk per m^3 of permeate with rotation speed for the two disks, using data of Figure 14.

values, but the permeate flux increase due to vanes being much larger than in UF of milk, the energy per m^3 of permeate in MF was smallest for the 6-mm vanes disk. A physical reason may be that, since, in the presence of vanes, the flux at high rotation speeds has not reached the mass-transfer regime in our tests (as seen from Figure 6), the benefit of increasing rotation speed is less than for the smooth disk which operates in the mass-transfer regime at pressures of the test. Of course, in an industrial module with a membrane on each side of the disk, the energy per m^3 of permeate will be half of that in our single membrane pilot.

Discussion and Conclusion

Our results demonstrate that the high performance of rotating disk filtration systems, observed by many authors in microfiltration, subsists in ultrafiltration. Tests performed with the stainless steel module confirmed that, at high rotation speed, the concentration polarization was considerably reduced as the permeate flux kept increasing until at least 1,000 kPa, especially when the disk was equipped with vanes.

Another important result is that, as in the case of microfiltration, the presence of vanes on the disk, which increases the fluid velocity and therefore the shear rate at the membrane, had a very important effect on fouling and on concentration polarization reduction and in permeate flux enhancement. However, flux enhancement due to the vanes was less than that observed in the MF of the cell or particulate suspensions (Brou et al., 2003). This difference could be due to the nature of the flux limiting phenomenon which, in MF, is mainly cake formation or to the absence of particles in milk.

In contrast to cross-flow filtration in tubular channels, the membrane shear stress cannot be measured from the pressure drop and has to be calculated using boundary layer theory in the case of a flat disk without vanes. Calculation of the shear stress in the presence of vanes would require the use of computing fluid dynamics (CFD) software, which was beyond the scope of this investigation. So, it was encouraging to find that the permeate fluxes obtained on using various types of disks and two different sizes modules were well correlated by a function of the same power of the membrane shear rate, using appropriate velocity coefficients for each type of disk. This result led us to postulate that mean membrane shear rate (or stress) is the main parameter governing permeate flux in these systems and details of internal flows are less important. If this simple result also holds for larger sizes than our prototypes, it would greatly simplify the design of industrial scale systems using Eq. 2b. This equation shows that increasing rotation speed has a slightly stronger effect than increasing the radius, because shear rate increases as $\omega^{1.8} r^{1.6}$ for same disk azimuthal velocity. In addition, larger diameter devices will present a more inhomogeneous permeate flux because of larger relative variations in shear rate between center and periphery.

Acknowledgments

This research has been supported in part by the CNRS-INRA Program Prosetia and by the Regional Council of Picardy. The large module was designed by R. Bouzerar and P. Paullier in our laboratory. The authors thank Alting Co. (Strasbourg) for supplying the membranes and P. Paullier for his technical assistance.

Notation

e = axial gap between flat disk and membrane, m
J = permeate flux, L $h^{-1} m^{-2}$
k = velocity factor
N = rotation speed, rpm
p = pressure, Pa
p_c = peripheral pressure, Pa
P_e = electrical power, W
P_{ev} = electrical power without fluid, W
P_m = mechanical power, W
P_N = net power ($P_e - P_{ev}$), W
p_o = pressure at the center of disk, Pa
Q_F = filtration flow rate, L h^{-1}
r = radius, m
R, R_d = housing inner radius, disk radius, m
R_1, R_2 = membrane inner, outer, radii, m
s = height of vanes, mm
T = temperature, °C
TMP, P_{tm} = mean transmembrane pressure, Pa
w = width of vanes, mm

Greek letters

γ_m = mean shear rate, averaged over area, s^{-1}
γ_{wt} = shear rate at membrane in turbulent regime, s^{-1}
ν = cinematic viscosity, $m^2 s^{-1}$
μ = fluid viscosity, Pa s
ρ = fluid density, kg m^{-3}
ω = angular velocity, rd s^{-1}

Literature Cited

Al-Akoum, O., L. H. Ding, and M. Y. Jaffrin, "Microfiltration and Ultrafiltration of UHT Skim Milk with a Vibrating Membrane Module," *Sep. Purif. Technol.*, **28**, 219 (2002a).

Al-Akoum, O., L. H. Ding, R. Chotard-Ghodsnia, and M. Y. Jaffrin, "Casein Separation from Skimmed Milk using a VSEP Dynamic Filtration Module," *Desalination*, **144**, 325 (2002b).

Al-Akoum, O., R. Chotard-Ghodsnia, L. H. Ding, and M. Y. Jaffrin, "Ultrafiltration of Low Heat and UHT Skim Milks with a Shear-Enhanced Vibrating Filtration System," *Sep. Sci. and Tech.*, **38**, 571 (2003).

Bouzaza, A. K., M. Y. Jaffrin, and B. B. Gupta, "Effect of Flow and Pressure Pulsations on Milk Ultrafiltration by Mineral Membranes," *Proc. of ICIM 89, 1st Int. Conf. on Inorg. Membranes*, Montpellier, France, 439 (July 3–6, 1989).

Bouzerar, R., M. Y. Jaffrin, L. H. Ding, and P. Paullier, "Influence of Geometry and Angular Velocity on Performance of a Rotating Disk Filter," *AIChE J.*, **46**, 265 (2000).

Bouzerar, R., M. Y. Jaffrin, P. Paullier, and P. Boulnois, "Dispositif de Filtration Dynamique," French Patent FR 63573M (July 5, 2001).

Brou, A., L. H. Ding, P. Boulnois, and M. Y. Jaffrin, "Dynamic Microfiltration of Yeast Suspensions Using Rotating Disks Equipped with Vanes," *J. Membr. Sci.*, **197**, 269 (2002).

Brou, A., M. Y. Jaffrin, L. H. Ding, and J. Courtois, "Microfiltration and Ultrafiltration of Polysaccharides Produced by Fermentation Using a Rotating Disk Dynamic Filtration System," *Biotech. and Bioeng.*, **82**, 429 (2003).

Dal-Cin, M. M., C. N. Lick, A. Kumar, and S. Lealess, "Dispersed Phase Back Transport during Ultrafiltration of Cutting Oil Emulsions with a Spinning Disc Geometry," *J. Membr. Sci.*, **141**, 165 (1998).

Ding, L. H., O. Al-Akoum, A. Abraham, and M. Y. Jaffrin, "Milk Protein Concentration by Ultrafiltration with Rotating Disk Modules," *Desalination*, **146**, 307 (2002).

Ernstrom, C. A., B. J. Sutherland, and G. W. Jameson, "Cheese Base for Processing. A High Yield Product from Whole Milk by Ultrafiltration," *J. Dairy Sci.*, **63**, 228 (1980).

Frenander, U., and A. S. Jönsson, "Cell Harvesting by Cross-Flow Microfiltration using a Shear-Enhanced Module," *Biotech. Bioeng.*, **52**, 397 (1996).

Gésan-Guiziou, G., O. Al-Akoum, L. H. Ding, E. Boyaval, G. Daufin, and M. Y. Jaffrin, "Stabilité de la Filtration Tangentielle de Lait Écrémé en Modes Tangentiels Classique et Vibrant," *IAA*, **119**(6), 10 (2002).

Grandison, A. S., W. Youravong, and M. J. Lewis, "Hydrodynamic Factors Affecting Flux and Fouling during Ultrafiltration of Skimmed Milk," *Le Lait*, **80**, 165 (2000).

Harscoat, C., M. Y. Jaffrin, R. Bouzerar, and J. Courtois, "Influence of Fermentation Conditions and Microfiltration Process on Membrane Fouling during Recovery of Glucuronane Polysaccharides from Fermentation Broths," *Biotech. Bioeng.*, **65**, 500 (1999).

Lee, S. S., A. Burt, G. Russotti, and B. Buckland, "Microfiltration of Recombinant Yeast Cells using a Rotating Disk Dynamic Filtration System," *Biotech. Bioeng.*, **48**, 386 (1995).

Lucas, D., M. Rabiller-Baudry, L. Millesime, B. Chaufer, and G. Daufin, "Extraction of α-Lactalbumin from Whey Protein Concentrate with Modified Inorganic Membranes," *J. Membr. Sci.*, **148**, 1 (1998).

Maubois, J. L., G. Moquot, and J. L. Thapon, "Preparation de Préfromage à Partir de Préfromage Liquide Obtenu par Ultrafiltration du Lait," *Le Lait*, **51**, 495 (1971).

Miralles, B., B. Bartolone, M. Ramos, and L. Amigo, "Determination of Whey Protein to Total Protein Ratio in UHT Milk using 4th Derivative Spectroscopy," *Int. Dairy J.*, **10**, 191 (2000).

Pessoa, A., and M. Vitolo, "Evaluation of Cross-Flow Microfiltration Membrane using a Rotary Disc-Filter," *Process Biochem.*, **33**, 39 (1998).

Schlichting, H., *Boundary Layer Theory*, 7th ed., McGraw-Hill, New York (1968).

Manuscript received Nov. 25, 2002, revision received Feb. 20, 2003, and final revision received Apr. 11, 2003.